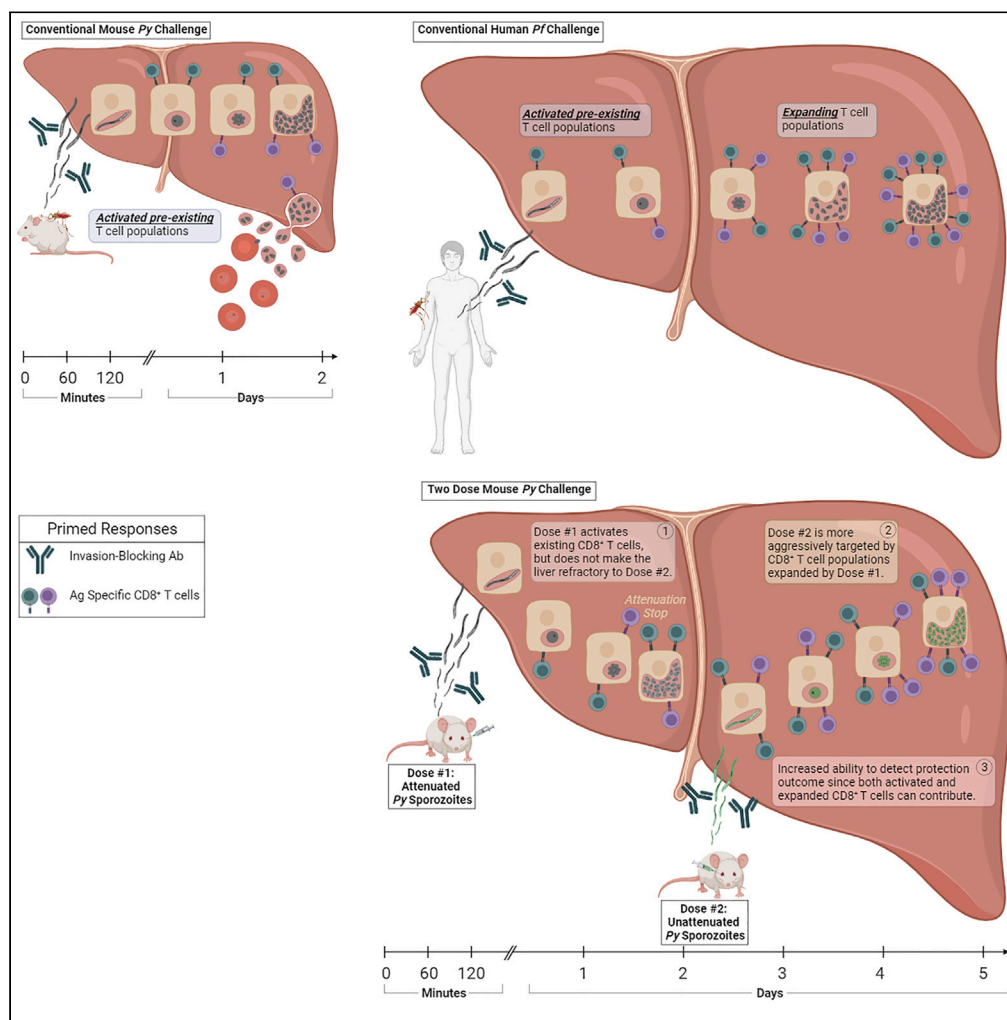


Article

# More time to kill: A longer liver stage increases T cell-mediated protection against pre-erythrocytic malaria



Naveen Yadav, Chaitra Parthiban, Zachary P. Billman, ..., Melanie J. Shears, Rebekah A. Reynolds, Sean C. Murphy

murphysc@uw.edu

**Highlights**

Longer malaria liver stage exposure highlights the role of CD8<sup>+</sup> T cells in protection

A two-dose challenge model in mice provides longer *Plasmodium* liver stage exposure

Vaccine-induced immunity is improved against the longer liver stage two-dose challenge



## Article

## More time to kill: A longer liver stage increases T cell-mediated protection against pre-erythrocytic malaria

Naveen Yadav,<sup>1,2</sup> Chaitra Parthiban,<sup>1,2</sup> Zachary P. Billman,<sup>1,2</sup> Brad C. Stone,<sup>1,2</sup> Felicia N. Watson,<sup>1,2</sup> Kevin Zhou,<sup>1,2</sup> Tayla M. Olsen,<sup>1,2</sup> Irene Cruz Talavera,<sup>1,2</sup> Annette Mariko Seilie,<sup>1,2</sup> Anya C. Kalata,<sup>1,2</sup> Jokichi Matsubara,<sup>1,2</sup> Melanie J. Shears,<sup>1,2</sup> Rebekah A. Reynolds,<sup>1,2</sup> and Sean C. Murphy<sup>1,2,3,4,\*</sup>

## SUMMARY

**Liver stage (LS) *Plasmodia* mature in 2–2.5 days in rodents compared to 5–6 days in humans. *Plasmodium*-specific CD8<sup>+</sup> T cell expansion differs across these varied timespans. To mimic the kinetics of CD8<sup>+</sup> T cells of human *Plasmodium* infection, a two-dose challenge mouse model that achieved 4–5 days of LS antigen exposure was developed. In this model, mice were inoculated with a non-protective, low dose of late-arresting, genetically attenuated sporozoites to initiate T cell activation and then re-inoculated 2–3 days later with wild-type sporozoites. Vaccines that partially protected against traditional challenge completely protected against two-dose challenge. During the challenge period, CD8<sup>+</sup> T cell frequencies increased in the livers of two-dose challenged mice but not in traditionally challenged mice, further suggesting that this model better recapitulates kinetics of CD8<sup>+</sup> T cell expansion in humans during the *P. falciparum* LS. Vaccine development and antigen discovery efforts may be aided by using the two-dose challenge strategy.**

## INTRODUCTION

Malaria is a tremendously burdensome infectious disease caused by *Plasmodium* parasites that are transmitted to humans by the bites of *Anopheles* mosquitoes. After *Plasmodium* sporozoites (spz) are transmitted by blood-feeding *Anopheles* mosquitoes, the spz migrate in the skin, enter blood vessels, and invade hepatocytes. Combatting these parasites in the pre-erythrocytic (PE) spz and liver stages (LS) involves humoral and cellular immune responses. Antibodies can block egress of *Plasmodium* spz from the skin and can prevent hepatocyte invasion.<sup>1</sup> Once a hepatocyte is infected, the ensuing LS is highly proliferative: one parasitized hepatocyte can produce tens of thousands of merozoites that will egress into the blood and initiate a blood-stage infection. Infected hepatocytes are specifically targeted and killed by cytotoxic CD8<sup>+</sup> T cells during the LS.<sup>2,3</sup> CD8<sup>+</sup> T cell responses in the liver are essential for spz vaccine-mediated sterile protection in mice<sup>4,5</sup> and non-human primates (NHP).<sup>6</sup> Long-term sterile protection in these pre-clinical animal models is associated with liver-targeted CD8<sup>+</sup> T cells called liver-resident memory CD8<sup>+</sup> T cells (Trm cells).<sup>7–10</sup> If host T cell responses fail to completely stop the parasite at the LS, the merozoites released from infected hepatocytes can initiate blood-stage infection, rendering ongoing T cell responses against LS antigens irrelevant to protection.

Murine models of PE *Plasmodium* infection are important for antigen discovery and pre-clinical evaluation of vaccines. However, critical differences in the duration of the LS in murine-versus human-infecting *Plasmodium* species would influence the outcome of cellular responses to LS parasites. Notably, while the human *P. falciparum* (Pf) LS takes up to six days to complete, murine-infecting *P. yoelii* (Py) and *Plasmodium berghei* (Pb) species complete the LS in 2–2.5 days (Figure 1). This is one of the most important but overlooked differences between human and murine models of malaria. Other important differences that could contribute to differences in outcomes between mice and humans include differences in parasite genetic and metabolic factors, variation in parasite-encoded antigens and immune system evasion-associated genes, and host immune system differences in inbred mice versus outbred humans especially as they relate to MHC restriction and TCR diversity.<sup>11–13</sup> However, murine and human models also have considerable similarities including at the level of the immune system, and parasite genetics,<sup>11,14,15</sup> making mouse models useful initial tools to study host-parasite interactions. In both mice and humans, vaccine-induced CD8<sup>+</sup> T cells are rapidly activated following antigen encounter,<sup>3,16</sup> but the difference in duration of the LS may potentially mean that the increasing pool of parasite-specific CD8<sup>+</sup> T cells may only be influencing the outcome in humans, not in mice. Expansion of antigen-specific CD8<sup>+</sup> T cells in lymphoid organs and their recruitment to sites of infection often takes more than two days.<sup>17–21</sup> Given this lag between

<sup>1</sup>Department of Laboratory Medicine and Pathology, University of Washington, Seattle, WA, USA

<sup>2</sup>Center for Emerging and Re-emerging Infectious Diseases, University of Washington, Seattle, WA, USA

<sup>3</sup>Department of Microbiology, University of Washington, Seattle, WA, USA

<sup>4</sup>Lead contact

\*Correspondence: [murphysc@uw.edu](mailto:murphysc@uw.edu)

<https://doi.org/10.1016/j.isci.2023.108489>



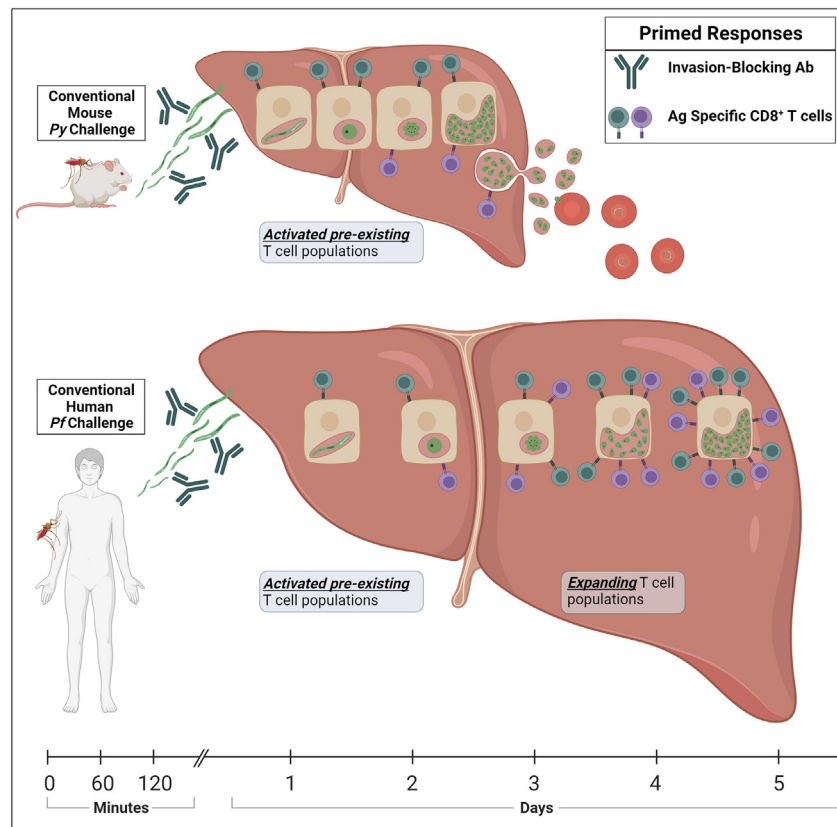


**Figure 1. Duration of mouse vs. human liver infection by *Plasmodium* parasites in relation to immune cell activation and parasite killing**

*Py* completes LS development (top) in mice in ~2–2.5 days during which T cells are activated in response to antigen exposure, but this is not enough time to significantly increase the T cell population. In contrast, *Pf* infection of human livers occurs over ~5–6 days (bottom). During this time, *Pf*-specific T cells both activate and increase in number to control the parasite *before* the LS completes. The contribution of activation and numeric expansion of T cells therefore differs in these hosts.

pathogen exposure and increases in CD8<sup>+</sup> T cell responses, it is possible that the true protective potential of CD8<sup>+</sup> T cells is not fully harnessed in the mouse *Plasmodium* LS infection model.<sup>22</sup> In mouse models, protection against spz challenge may rely mainly on pre-existing parasite-specific CD8<sup>+</sup> T cells present in liver, while in the case of humans, participation from numerically expanded CD8<sup>+</sup> T cells is also expected. Given these differences in *Plasmodium* biology, we hypothesize that some potentially protective *Plasmodium*-derived antigens may have been hiding in plain sight by being categorized as non-protective in traditional murine vaccine challenge studies.

We speculated that the difference in duration of LS between *Py/Pb* and *Pf* is the reason that murine models of malaria require very high T cell frequencies to achieve sterile protection against the PE stage.<sup>23–25</sup> Therefore, if the duration of the *Py* LS could be extended in immunocompetent mice to more closely mimic the length of the *Pf* LS, the full contribution of T cell activation, trafficking, numeric expansion, and effector functions could be harnessed. Humanized mouse models permit infection with *Pf* spz and achieve a 5–6 days LS, but such mice are immunocompromised and thus cannot currently be used to evaluate cellular immunity.<sup>26</sup> We therefore developed a simple immunocompetent mouse model using *Py* that more closely approximates the duration of the *Pf* LS. This model uses a serial two-dose spz inoculation to extend the duration of mouse LS exposure so that the complete effects of memory T cells can be measured. Our “two-dose challenge” combines an initiating low “dose #1” ( $2 \times 10^3$ ) of late-arresting, genetically attenuated *Py*-FabB/F-deficient spz (*Py*-FabB/F)<sup>27</sup> followed two days later by “dose #2” ( $2.5 \times 10^2$  to  $1 \times 10^3$  depending on the mouse strain) of wild-type *Py* spz (*Py*-WT) (Figure 2). This approach might better evaluate the true potential efficacy of pre-clinical candidate vaccines.

We investigated and compared the protective outcomes of the conventional one-dose challenge vs. our novel serial two-dose challenge in mice. We evaluated two different vaccine approaches currently used for examination of vaccine candidates against malaria: [1] radiation-attenuated spz (RAS) and [2] DNA prime-and-RAS trap vaccination. Innate immune responses were also studied during the two serial doses in naive and vaccinated mice to determine whether innate responses elicited by dose #1 were affecting dose #2. CD8<sup>+</sup> T cell responses were tracked throughout the LS to monitor T cell activation and numeric expansion kinetics following one- or two-dose challenges. Protection was enhanced by two-dose challenge compared to one-dose challenge in vaccinated mice and CD8<sup>+</sup> T cells were critical for the enhanced protection. T cell response kinetics indicated that memory T cell responses underlie the difference in protection observed. Additionally, innate

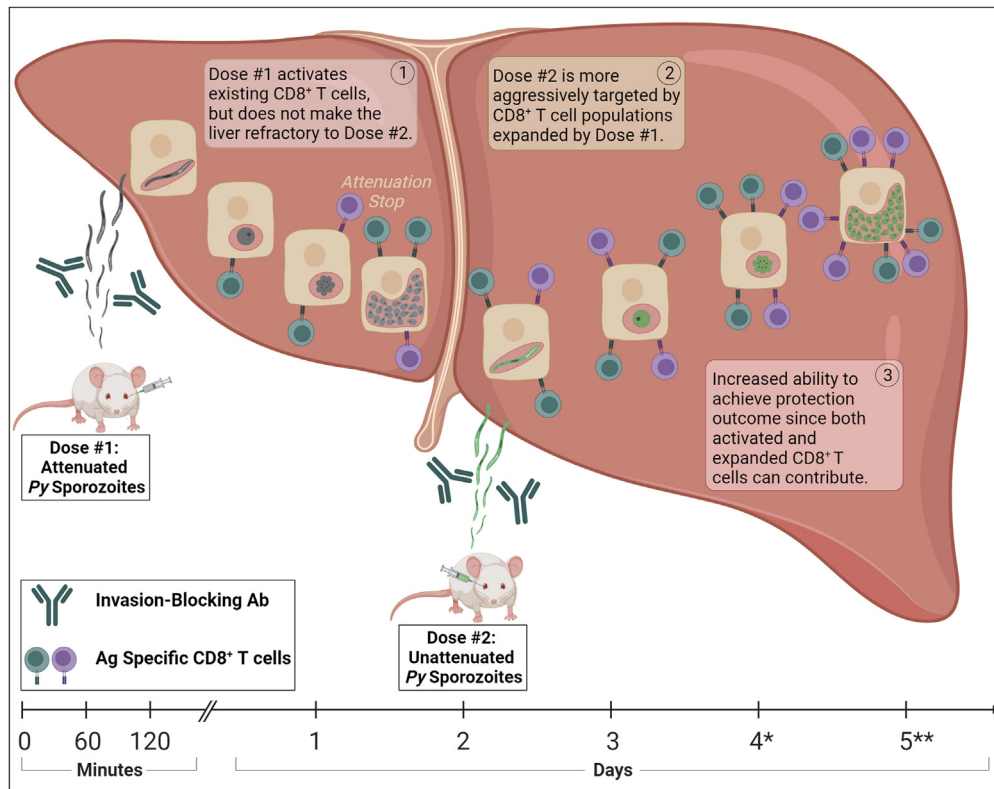


**Figure 2. Two-dose challenge model of extended duration LS infection in mice**

During a two-dose challenge, mice received the first dose of Py-FabB/F spz (dose #1) on day 0 followed by the second dose of Py-WT spz (dose #2) on day 2. Dose #1 re-activates adaptive immune responses induced by prior vaccination. Antibodies can act before the parasite can reach the liver, whereas during LS infection activated T cells have a role. Vaccination-induced T cells will be the first to be activated after initial dose and will start killing the parasite antigen-expressing cells. On day 2, upon challenge with Py-WT spz, the activated and now increasing CD8<sup>+</sup> T cells are better able to kill parasite-infected hepatocytes.

immune responses generated by the dose #1 did not affect infectivity of the challenge dose (dose #2). Since *Pf* in humans operates on a similar duration to that of two-dose challenge in mice, this model may be harnessed to understand the cellular immune response and discover antigens to achieve better and more protective outcomes.

## RESULTS

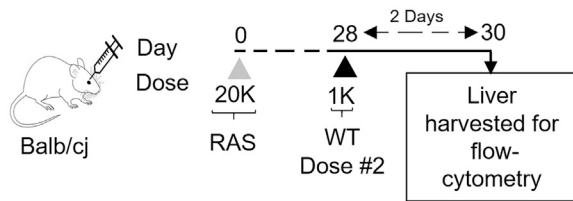
### Activation and numeric expansion of CD8<sup>+</sup> T cell responses against *Plasmodium* antigens over the period of time

To correlate the activation and numeric expansion of CD8<sup>+</sup> T cell responses with the duration of exposure to liver-stage antigens, we tracked the kinetics of liver CD8<sup>+</sup> T cell responses in Py-RAS immunized mice on days 2–4 post-challenge (Figures 3A and 3B). CD8<sup>+</sup> T cells were measured by flow cytometry (Figures 3C, 3D, and S1) in the liver of conventionally challenged mice on day 2 (Figure 3A) and Py-Fabfbf challenged mice on day 4 (Figure 3B). Activated CD8<sup>+</sup> T cells were present in the livers of immunized mice at both time points (Figures 3E–3H). However, increased numbers of activated CD8<sup>+</sup> T cells were only observed on day 4, including those expressing CD69 and KLRG-1 (Figure 3E), which are known to play important roles in protecting the liver against *Plasmodium* spz challenge.<sup>7,28</sup> Further flow cytometry analyses were performed to examine memory CD8<sup>+</sup> T cells (total memory [Tm], central memory [Tcm], and effector memory [Tem]) and their activation status (CD69 and KLRG-1 expression) (Figures 3F–3H).

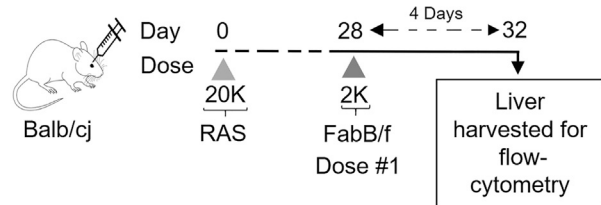
As expected, the number of CD44<sup>Hi</sup>/Tm cells was significantly reduced in livers on day 2, but increased by day 4 (Figure 3F), consistent with activation and cell recruitment and/or expansion kinetics of CD8<sup>+</sup> Tm/CD44<sup>Hi</sup> cells over the course of infection.<sup>17–21</sup> Tcm cells were also reduced on day 2 and remained low on day 4 (Figure 3F). To ascertain that Tcm cells were getting activated, we examined their activation phenotype cell surface markers CD69 and KLRG-1 and found increases in the frequency of activated Tcm cells upon challenge. As predicted, high frequencies of activated Tcm cell populations were seen by day 4 (Figure 3G). Tem/Teffector (Te) cells are capable of cytotoxic killing of parasites in the liver.<sup>3</sup> Thus, we examined Tem/Te cell frequencies and activation status on days 2 and 4. Interestingly, the frequencies of Tem/Te cells did not increase in the liver on day 2, but did significantly increase by day 4 (Figure 3F). We did not observe further increases in activated phenotype Tem cells in livers on day 2, but by day 4 we could see significantly higher numbers of those cells (Figure 3H). Thus, there is an increased CD8<sup>+</sup> T cell population in the liver of mice four days after initial challenge only.

**Immunization strategy**

**A WT challenge**

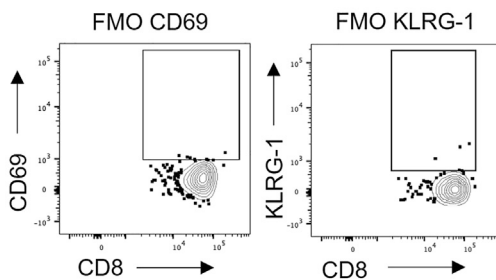


**B FabB/f challenge**

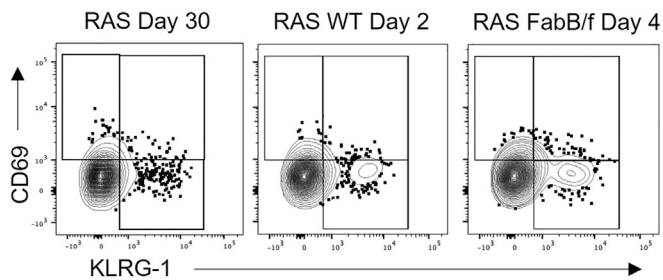


**Characterization of activated phenotype CD8<sup>+</sup> T cells in immunized and/or challenged mice liver**

**C FMO controls for activation markers**

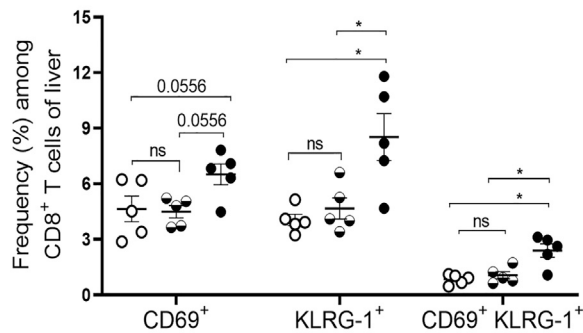


**D Activation phenotype CD8<sup>+</sup> T cells in immunized mice**

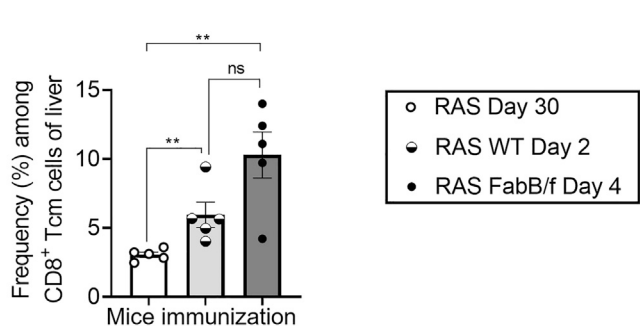


**Activation phenotype CD8<sup>+</sup> T cell kinetic data for two- vs. four-days challenged mice liver**

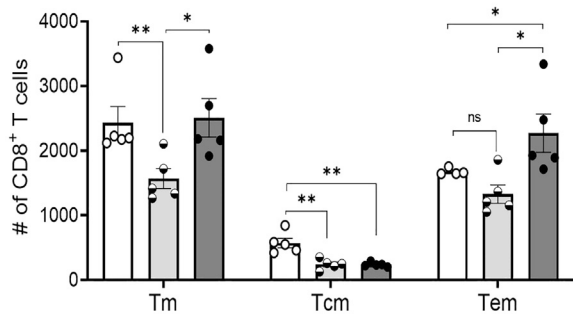
**E Activation phenotype CD8<sup>+</sup> T cell population**



**G CD69<sup>+</sup> KLRG-1<sup>+</sup> Tcm cells**



**F Memory CD8<sup>+</sup> T cell numbers**



**H CD69<sup>+</sup> KLRG-1<sup>+</sup> Tem/Te cells**

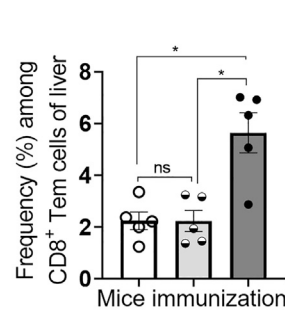


**Figure 3. Kinetics of CD8<sup>+</sup> T cell responses in one-dose Py-WT and Py-FabB/F challenged mice**

BALB/cj mice were vaccinated 28 days earlier with  $2 \times 10^4$  Py-RAS and were subjected to either (A) WT or (B) Py-FabB/F challenge followed by liver harvest on days depicted in the figure to study the activated CD8<sup>+</sup> T cell kinetics by flow cytometry.

**Figure 3. Continued**

- (C) Representative contour plots for CD69 and KLRG-1 FMO (fluorescence minus one) controls for positive gating of cells.
- (D) Representative contour plots for activation phenotype of CD8<sup>+</sup> T cells (CD69<sup>+</sup>, KLRG-1<sup>+</sup> and CD69<sup>+</sup> KLRG-1<sup>+</sup>) in the liver of differently immunized mice as depicted in the figure.
- (E) Frequency (%) of CD69<sup>+</sup>, KLRG-1<sup>+</sup> and CD69<sup>+</sup> KLRG-1<sup>+</sup> cells among CD8<sup>+</sup> T cells in livers of mice immunized as depicted in A.
- (F) Numbers of memory CD8<sup>+</sup> T cells normalized to 2x10<sup>4</sup> CD8<sup>+</sup> T cell numbers, total memory (Tm) i.e., CD44<sup>Hi</sup>/CD8<sup>+</sup> T cells, and central memory (Tcm) and effector memory (Tem) in Tm population.
- (G) Tcm and (H) Tem cells among CD8<sup>+</sup> T cell population were tracked for the frequency (%) of CD69<sup>+</sup> KLRG-1<sup>+</sup> cells in the liver of mice groups differently immunized mice as depicted in the figure. N = 5 mice per group. Data are representative from two independent experiments. Data are the mean ± SEM. Data were analyzed by Mann-Whitney test. p < 0.05 is considered significant. \*p < 0.05, \*\*p < 0.01.

**Two-dose challenge model for extended liver-stage antigen exposure and kinetics of CD8<sup>+</sup> T cell responses**

To mimic human *Plasmodium* LS challenge and to take advantage of numerically expanding CD8<sup>+</sup> T cells, we developed a “two-dose challenge” model in mice. In this model, two serial subsequent doses of spz are inoculated into mice. The initiating low “dose #1” consists of 2x10<sup>3</sup> late-arresting, genetically attenuated *Py*-FabB/F-deficient spz (*Py*-FabB/F) followed two days later by “dose #2” of wild-type *Py* spz (*Py*-WT) at 2.5x10<sup>2</sup> to 1x10<sup>3</sup> spz depending on the mouse strain (Figure 2). Dose #1 of *Py*-FabB/F is intended to initiate activation and expansion of CD8<sup>+</sup> T cells, as described above in Figure 3, whereas dose #2 of *Py*-WT evaluates protection rendered by the activated and numerically expanding CD8<sup>+</sup> T cell responses. When mice were vaccinated with RAS and subjected to one- or two-dose challenge four weeks later (Figures 4A and 4B), CD8<sup>+</sup> T cells were activated and numerically expanded in the two-dose challenged mice by four days (Figures 4C–4E), similar to numeric expansion observed with the *Py*-FabB/F dose alone by day 4 (Figures 3E, 3G, and 3H).

Naturally developing and boosting of CD8<sup>+</sup> T cell responses against WT LS parasites in humans is difficult.<sup>29</sup> As such, we next considered whether the *Py*-FabB/F attenuated parasite in dose #1 of our two-dose challenge might more efficiently reactivate CD8<sup>+</sup> T cells than *Py*-WT (Figure 4B). However, *Py*-WT and *Py*-FabB/F challenged mice showed similar CD8<sup>+</sup> T cell numeric expansion (Figures 4C–4E). These observations demonstrate that LS infection by both attenuated and unattenuated parasites activates RAS-primed memory CD8<sup>+</sup> T cells responses.

To investigate immune activation by dose #1, we evaluated the type I interferon response pathway, which is known to coincide with the early activation of T cells.<sup>30</sup> For tracking, we studied expression of type I interferon-stimulated genes (ISGs) 42–44 h after dose #1 (2x10<sup>3</sup> *Py*-FabB/F) of the two-dose challenge by qRT-PCR (*Ifit1* and *Ifit44* normalized to mouse GAPDH) in RAS-vaccinated mice (Figure 4F).<sup>31,32</sup> Interestingly, ISG expression was significantly increased in *Py*-RAS immunized mice after the dose #1 (2x10<sup>3</sup> *Py*-FabB/F) (Figure 4G) before they received wild type spz challenge dose #2. Activation of antigen-specific CD8<sup>+</sup> T cells in *Py*-RAS immunized mice by dose #1 may serve as the source for accelerated ISG expression. This ISG data concurs with our flow cytometry data on CD8<sup>+</sup> T cell activation at day 2 after dose #1 (Figures 4C and 4D). Thus, it could be concluded that for lengthened LS antigen exposure periods, higher activation and numeric expansion of CD8<sup>+</sup> T could be expected in the liver.

**Exposure to a low dose of *Py*-FabB/F spz does not reduce the liver burden of a subsequent wild-type spz challenge in naive mice**

To test whether infectivity was retained by dose #2 in the two-dose challenge model, we tested whether dose #1 conferred an inhibitory effect on the growth of wild type spz after dose #2. Liver burden after dose #2 was measured in naive BALB/cJ mice that received either a single challenge of 5x10<sup>4</sup> *Py-luc*-WT spz or the two-dose challenge (2x10<sup>3</sup> *Py*-FabB/F spz at 0 h followed by 5x10<sup>4</sup> *Py-luc*-WT spz at 48 h) (Figures 5A and 5B). *In-vivo* imaging (IVIS) of luciferase-expressing parasites in the liver showed that there was no difference in the liver burden between the groups (Figures 5C and 5D). Both groups of mice also displayed similar times to patent blood-stage infection, with onset of blood stage infection on day 4 post-spz challenge that reached 1% parasitemia on day 5 (Figure 5E). Also, we did not observe delayed patency for blood-stage infection for mice undergoing one-dose (1x10<sup>3</sup> *Py-luc*-WT spz) versus two-dose challenge (2x10<sup>3</sup> *Py*-FabB/F spz at 0 h followed by 1x10<sup>3</sup> *Py-luc*-WT spz at 48 h) (Figure S2A). Furthermore, with 18S rRNA RT-PCR also we did not observe any significant reduction of the parasite load in the liver of challenge dose #2 (2x10<sup>4</sup>) after the dose #1 (2x10<sup>3</sup>) in naive mice (Figure S2B).

High doses of wild-type or late-arresting *Py* and *Pb* spz (≥5x10<sup>4</sup>) are known to activate type I IFN-stimulated responses in mice that render the liver refractory to immediate secondary infections.<sup>31,32</sup> Compared to these prior publications, the two-dose challenge model described herein uses a very low dose #1 (2x10<sup>3</sup>), which we hypothesized was not a strong innate immune trigger compared to higher doses. To test this, we measured the mRNA expression of ISGs<sup>31,32</sup> 42–44 h after dose #1 of the two-dose challenge by qRT-PCR (*Ifit1* and *Ifit44* normalized to mouse GAPDH) (Figure 5F). The dose #1 of 2x10<sup>3</sup> *Py*-FabB/F did not significantly increase ISG responses compared to the baseline of naive mice (Figure 5G). This lack of ISG induction is in stark contrast to the strong responses triggered by 5x10<sup>4</sup> *Py*-FabB/F or *Py*-WT spz (Figure 5G). Thus, it could be concluded that the infectivity of the wild type spz (dose #2) is maintained in the two-dose challenge model.

**A single vaccination with RAS confers complete protection against two-dose challenge**

Whole parasite vaccine (WPV) approaches are considered the gold standard for studying the completely protective CD8<sup>+</sup> T cell-mediated response against LS infection and thus are at the center of developing novel vaccine strategies and searching for new candidate antigens. Existing WPV strategies require intravenous (IV) administration of multiple doses of live-attenuated, infectious parasites in the host (mouse, NHP, or human), which complicate vaccine deployment.<sup>6,8,9,23</sup> For WPV approaches, strategies that achieve sterile protection with fewer doses are desirable. Pre-clinical animal models are critical for development of such efforts, especially if the model could more closely mimic

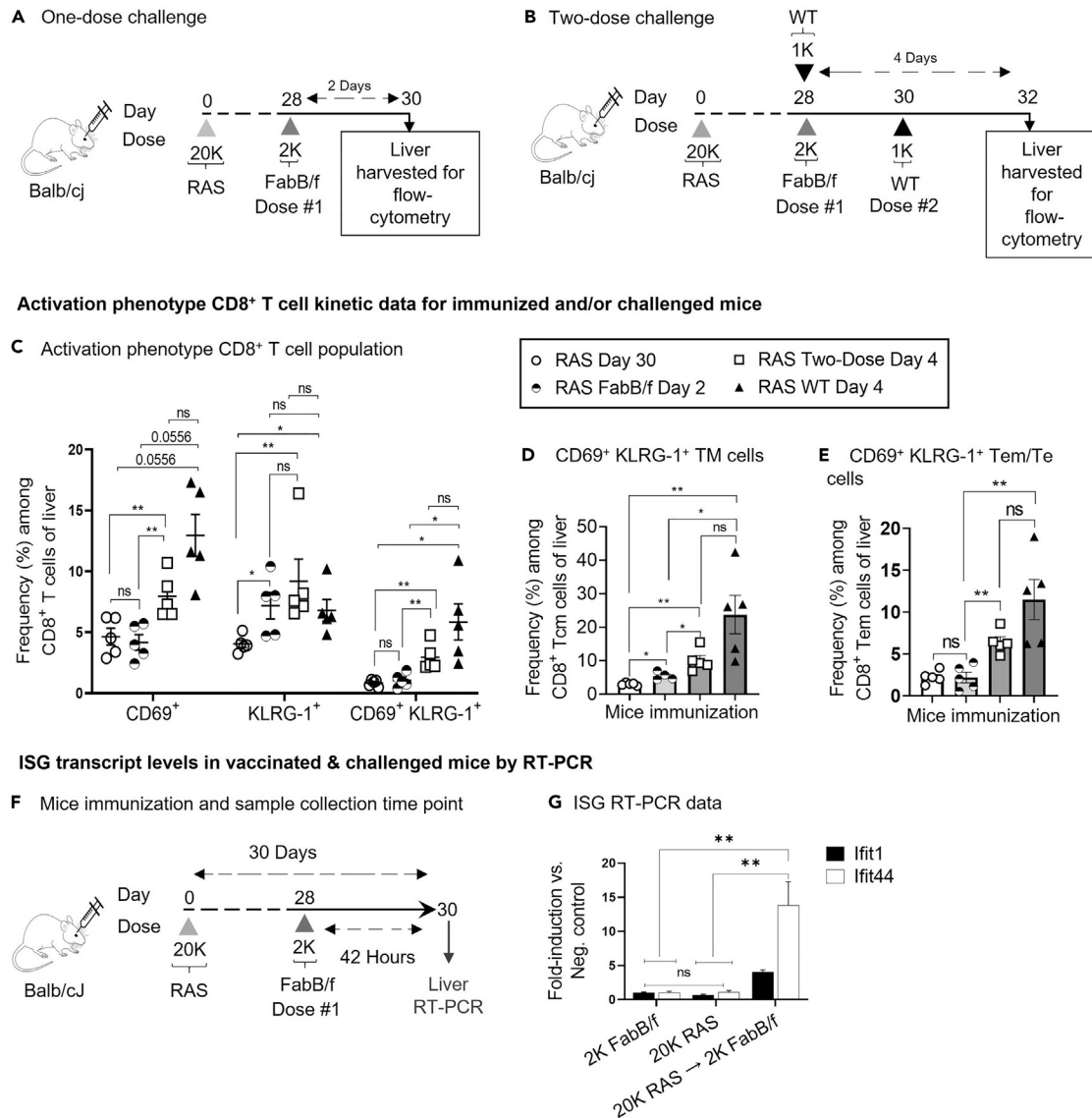


**Figure 4. Comparison of kinetics of CD8<sup>+</sup> T cell responses in one-versus two-dose challenged mice**

BALB/cj mice were vaccinated 28 days earlier with  $2 \times 10^4$  Py-RAS and were subjected to either (A) one- or (B) two-dose challenge followed by liver harvest on days depicted in the figure to study the activated CD8<sup>+</sup> T cell kinetics by flow cytometry. For one-dose challenges, mice were given either Py-FabB/F or Py-WT as noted in the subsequent data.

(C) Graph depicted frequency (%) of CD69<sup>+</sup>, KLRG-1<sup>+</sup> and CD69<sup>+</sup> KLRG-1<sup>+</sup> cells among CD8<sup>+</sup> T cell population in the liver of mice groups differently immunized mice as depicted in figure.

(D) Tcm and (E) Tem cells among CD8<sup>+</sup> T cell population were tracked for the frequency (%) of CD69<sup>+</sup> KLRG-1<sup>+</sup> cells in the liver of mice groups differently immunized mice as depicted in the figure.

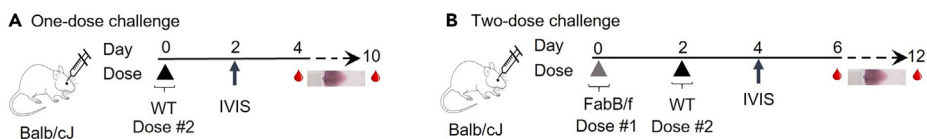
(F) Py-RAS immunized mice were injected with Py-FabB/F before taking out liver for RT-PCR to evaluate the effect of immunization on innate immune genes, *Ifit1* and *ifit44*.

(G) In mice previously exposed to a dose of  $2 \times 10^4$  Py-RAS, a significant increase in type I IFN response 42 h post-Dose #1 ( $2 \times 10^3$  Py-FabB/F). N = 5 mice per group. Data representative of two independent experiments. Data are the mean  $\pm$  SEM. Data were analyzed by Mann-Whitney test.  $p < 0.05$  is considered significant. \* $p < 0.05$ , \*\* $p < 0.01$ .

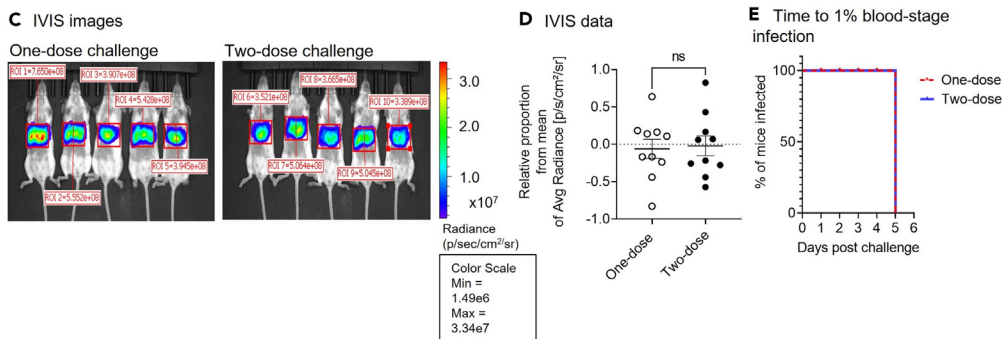
*Pf* infection and the responding CD8<sup>+</sup> T cell responses observed in human hosts. With this in mind, we explored protective outcomes in the LS two-dose challenge model compared to the conventional one-dose challenge in mice.

We assessed protection one month after a single dose of RAS, a well-established WPV strategy. Female BALB/cj and C57BL/6 mice were immunized IV with  $2 \times 10^4$  Py-RAS and assessed for protection by thin blood smear 28 days later by one- or two-dose challenge

**Mice immunization strategy and IVIS time point**



**Parasite liver load by IVIS imaging**



**ISG transcript levels in naïve challenged mice by RT-PCR**

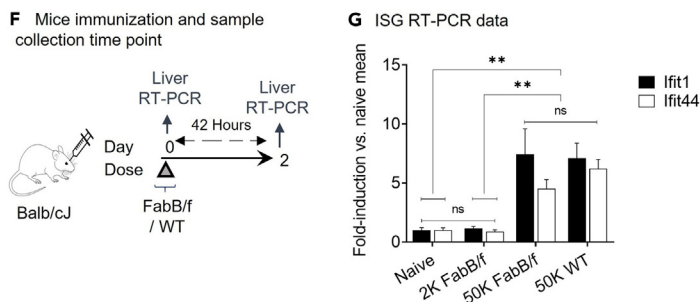


**Figure 5. The two-dose challenge model does not reduce the infectivity of the challenge dose in malaria-naïve mice**

BALB/cJ mice were inoculated either with (A) one- or (B) two-dose to compare parasite burden in liver by different strategies. (C) Individual mice imaged by IVIS after one-dose ( $5 \times 10^4$  [50K]) or two-dose challenge (dose #1 =  $2 \times 10^3$  [2K] Py-FabB/F, dose #2 =  $5 \times 10^4$  Py-Luc) and (D) their relative proportional mean radiance by IVIS in the liver. (E) Survival curve for 1% blood smear positivity of naïve mice after one- or two-dose challenge. (F) Naïve were injected with Py-FabB/F to evaluate dose #1 ( $2 \times 10^3$  Py-FabB/F) for induction of innate immune genes, *Ifit1* and *Ifit44* expression in liver by RT-PCR. (G) Dose #1 ( $2 \times 10^3$  Py-FabB/F) does not induce strong type I interferon responses at 42 h in naïve mouse livers (RT-PCR for *Ifit1* and *Ifit44* shown). Control groups mice injected with higher dose ( $5 \times 10^4$ ) Py-FabB/F or Py-WT induce strong type I interferon responses at 42 h in naïve mouse livers (RT-PCR for *Ifit1* and *Ifit44* shown). N = 5 mice/group. Data are from two independent experiments. Data are the mean  $\pm$  SEM. Data were analyzed by Mann-Whitney test.  $p < 0.05$  is considered significant. \*\* $p < 0.01$ .

(Figures 6A and 6B). For each mouse strain, four groups ( $n \geq 10$ /group) of immunized mice underwent a challenge dose #1 ( $2 \times 10^3$  Py-FabB/F spz) followed 48 h later by a wild-type (WT) dose #2 ( $1 \times 10^3$  Py-WT in BALB/cJ or  $2.5 \times 10^2$  Py-WT in C57BL/6) (Figures 6A and 6B). In the BALB/cJ strain, 80–100% of mice immunized with one dose of  $2 \times 10^4$  irradiated Py-RAS were protected in the two-dose challenge but only 40% were protected against the one-dose challenge (Figure 6C). One-dose of  $1-2 \times 10^4$  Py-RAS rarely protects more than half of BALB/cJ mice.<sup>10,33</sup> In addition, all naïve mice were infected after one or two dose challenge, indicating that dose #1 did not confer any protection against dose #2.

In C57BL/6 mice, there was partly enhanced protection against two-dose challenge compared to one-dose challenge on this schedule (Figure 6D). This strain of mice has been extremely difficult to completely protect against Py challenge by virtue of CD8<sup>+</sup> T cells, even after multiple doses of Py-RAS.<sup>33</sup> To evaluate if an additional day between dose #1 and dose #2 provided sufficient time for a protective response to develop, we repeated this experiment in C57BL/6 mice but administered dose #2 ( $2.5 \times 10^2$  Py-WT spz) three days after dose #1 ( $2 \times 10^3$  Py-FabB/F spz), thereby extending the total LS duration to five days (Figure 6E). With the three-day interval, 100% of C57BL/6 mice were protected against two-dose challenge, while none of the naïve mice were protected against this challenge (Figure 6F). These data suggest that extending the LS duration with the two-dose challenge model better harnesses the full protective capabilities of the WPV approach.



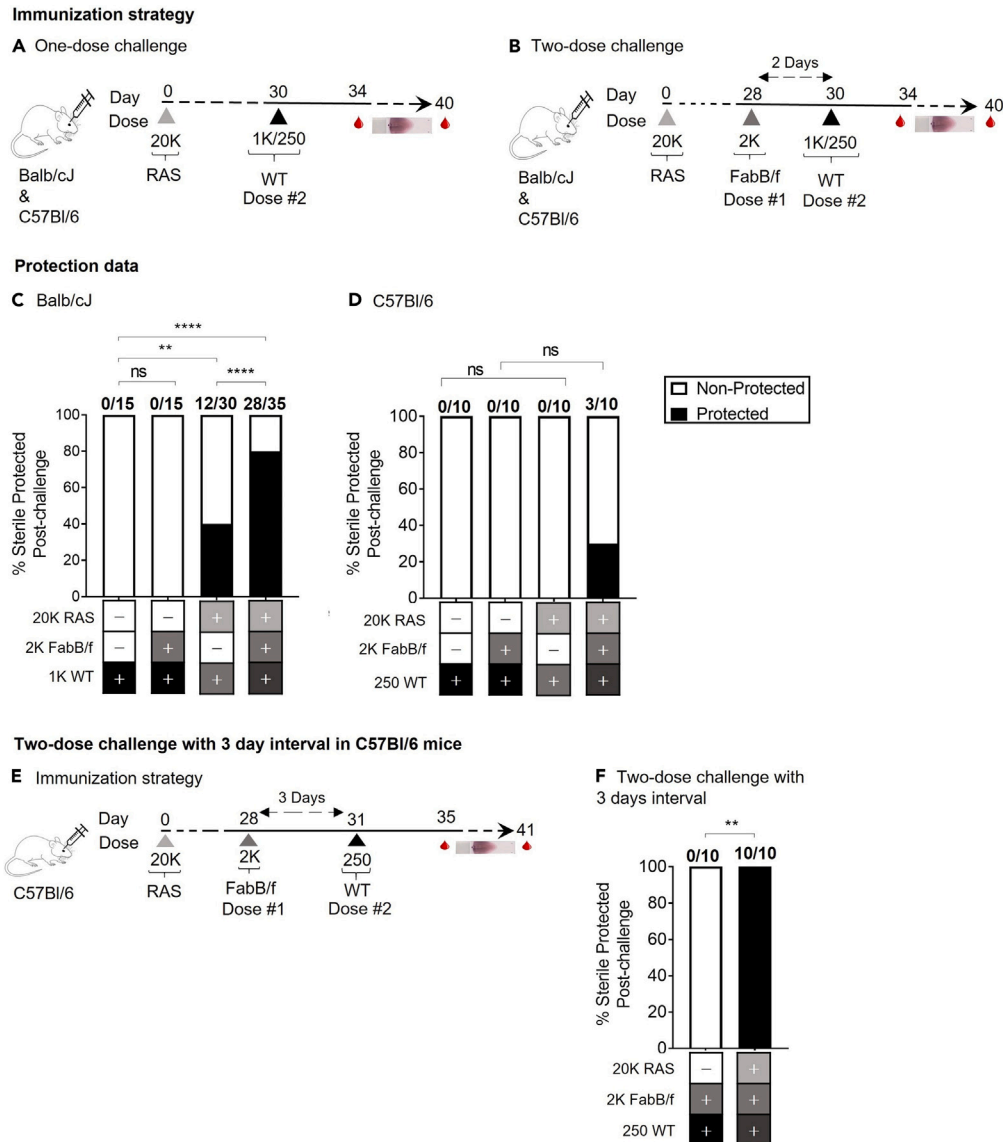


**Figure 6. WPV approach and protection in mice by one-dose vs. two-dose challenge**

BALB/cJ and C57BL/6 mice were either vaccinated 28 days earlier with  $2 \times 10^4$  Py-RAS or naive mice were subjected to (A) one- or (B) two-dose challenge (dose #1 =  $2 \times 10^3$  Py-FabB/F, dose #2 =  $1 \times 10^3$  [1K] Py-WT spz in BALB/cJ mice or  $2.5 \times 10^2$  [250] Py-WT spz in C57BL/6) followed by blood smears to evaluate for sterile protection. (C) Vaccinated BALB/cJ mice subjected to one-dose challenge have showed 0–40% protection, while the mice given two-dose challenge showed 80–100% protection, whereas all the naive mice challenged either with one-dose or two-dose came down with infection.

(D) On the other hand, vaccinated or naive C57BL/6 mice subjected to one-dose or two-dose challenge with two days interval between doses #1 and #2 showed 0% protection.

(E) In C57BL/6 mice, two-dose challenge was done with a three-day interval between dose #1 and #2 followed by blood smears.

(F) Increasing the interval between doses #1 and #2 to three days protected all mice, whereas all the naive mice challenged same way came down with infection. N  $\geq 10$  mice/group. Data compiled from two or more independent experiments. Data were analyzed by Fisher's exact test:  $p < 0.05$  is considered significant.

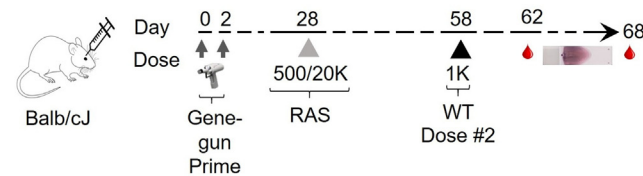
\* $p < 0.05$ , \*\* $p < 0.005$ , \*\*\*\* $p < 0.0001$ .

### Less stringent requirements for protection against two-dose challenge after prime-and-trap vaccination

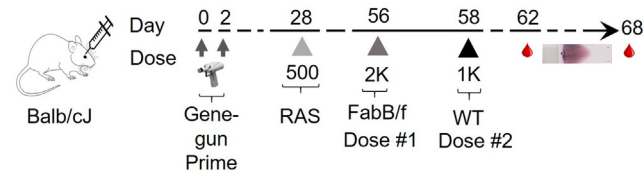
The prime-and-trap vaccine approach is a rationally-designed vaccine strategy intended to induce durable protective liver Trm cell responses.<sup>7,28,34</sup> Priming induces strong peripheral CD8<sup>+</sup> T cell responses followed by a 'trap' to pull the T cells into the liver to generate liver Trm cells. The trapping dose can be achieved using liver homing subunit vaccines or Py-RAS.<sup>28</sup> Here, mice were immunized using the prime-and-trap vaccine strategy followed by one- or two-dose challenge. The prime-and-trap vaccine consisted of a Py-CSP DNA priming dose delivered via gene gun followed one month later by a low trapping dose of Py-RAS (Figures 7A and 7B).

**Immunization strategy**

**A One-dose challenge**

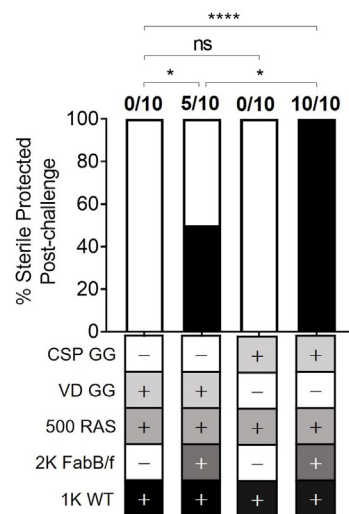


**B Two-dose challenge**



**Protection data**

**C 500 *Py*-RAS trap & one- vs. two-dose challenge**



**D Trap-dose escalation for one-dose challenge**

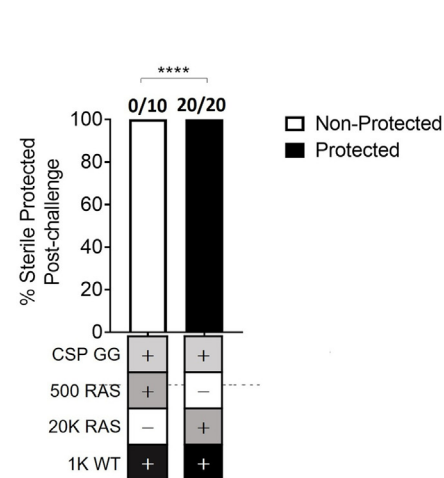


**Figure 7. Prime-trap vaccine approach and protection in mice by one- vs. two-dose challenge**

BALB/cJ mice were cluster primed with DNA encoding the *Py* circumsporozoite protein (*Py*-CSP) at days 0 and 2 with gene-gun technique. On day 28, mice were given a dose of *Py*-RAS  $5 \times 10^2$  [500] or  $2 \times 10^4$  via the IV route to boost and recruit CD8<sup>+</sup> T cells in liver. Finally, mice were subjected to either (A) one- ( $1 \times 10^3$  *Py*-WT) or (B) two-dose ( $2 \times 10^3$  *Py*-FabB/F then  $1 \times 10^3$  *Py*-WT) challenge on days 56 and 58 as shown followed by blood smears to evaluate for sterile protection. Control group mice received empty vector DNA immunization via gene-gun, a dose of *Py*-RAS and then subjected to either one-dose or two-dose challenge.

(C) All the mice of control and *Py*-CSP immunized group challenged with one-dose came down with infection, while in two-dose challenged mice control group were partially protected whereas the *Py*-CSP immunization fully-protected the group.

(D) Increasing the dose of *Py*-RAS trap in one-dose challenged mice groups also improved the protection in them,  $5 \times 10^2$  non-protective, and  $2 \times 10^4$  fully protective.  $N \geq 10$  mice/group. Data compiled from two or more independent experiments. Data were analyzed by Fisher's exact test:  $p < 0.05$  is considered significant. \* $p < 0.05$ , \*\*\*\* $p < 0.0001$ . VD, vector DNA (control).

BALB/cJ female mice were primed via gene gun with *Py*-CSP DNA on Day 0 and 2 followed by a single low trapping dose of  $5 \times 10^2$  *Py*-RAS on day 28 (Figures 7A and 7B). The  $5 \times 10^2$  *Py*-RAS dose is a mouse-to-human scaled dose intended to correspond to weight normalized human dose that does not protect mice on its own against standard one-dose challenge.<sup>3</sup> Control mice received nothing, gene gun priming only on day 0–2, or *Py*-RAS only on day 28. All mice were challenged on day 56 with either one- or two-dose challenge (Figures 7A and 7B). Prime-and-trap vaccinated mice were completely protected following a two-dose challenge but not a one-dose challenge (Figure 7C). Additionally, *Py*-RAS ( $5 \times 10^2$ ) alone provided sterile protection in a portion of mice undergoing two-dose challenge (Figure 7C), consistent with

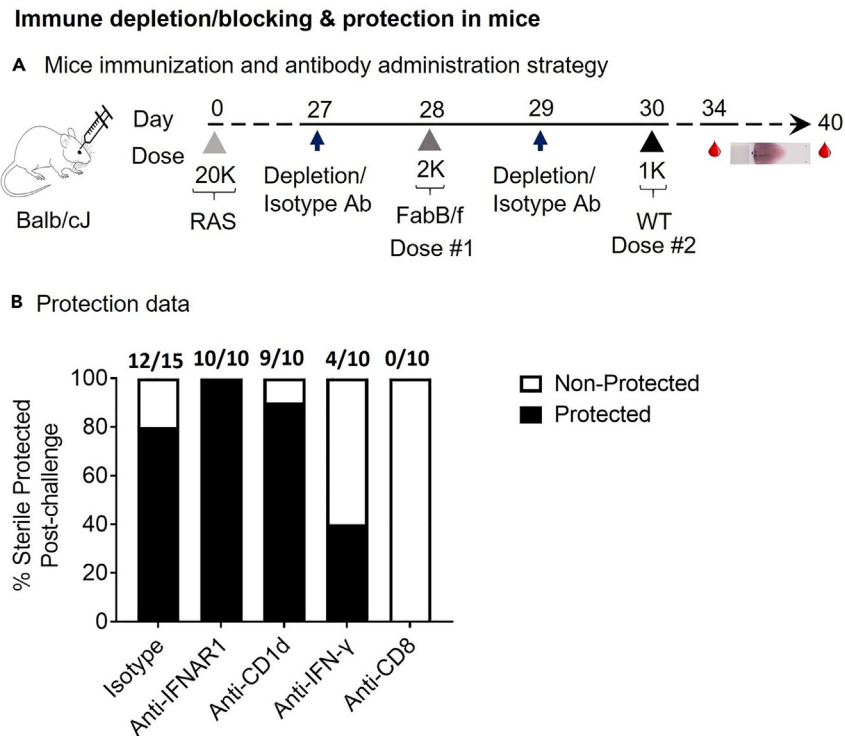


**Figure 8. Innate and adaptive immune responses participation in protection by two-dose challenge**

(A) The role of innate and adaptive immune cells and cytokine in protection by two-dose challenge model was evaluated using depletion/blocking strategy. BALB/cJ mice were vaccinated 28 days earlier with  $2 \times 10^4$  Py-RAS and were subjected to two-dose challenge. They were injected either depletion/blocking antibodies in test animals or isotype antibodies in control animals followed by blood smears to evaluate for sterile protection.

(B) All mice injected with anti-CD8 $\alpha$  mAb and 60% of those receiving anti-IFN- $\gamma$  mAb injected mice were positive for blood stage infection, while all mice injected with anti-CD1d and anti-IFNAR1 mAbs were protected. 80–100% of control mice injected with isotype control Abs were protected. Data were compiled and presented.

what was seen for higher dose of  $2 \times 10^4$  in Py-RAS-only vaccination presented earlier (Figure 6C). From this data, we concluded that RAS-only and prime-and-trap vaccine strategies are more protective with a two-dose challenge vs. a one-dose challenge.

The amount of the Py-RAS trapping dose in prime-and-trap leads to dose-dependent increases in liver CD8 $^+$  Trm cell frequencies, with fewer Trm cells expected after a  $5 \times 10^2$  Py-RAS trapping dose compared to higher trapping doses of  $1\text{--}2 \times 10^4$  Py-RAS.<sup>10,28</sup> Thus, we next determined if protection was improved by recruiting more CD8 $^+$  T cells to the liver in the one-dose challenge model when the trapping dose was increased from  $5 \times 10^2$  to  $2 \times 10^4$  Py-RAS (Figure 7A). Increasing the dose of Py-RAS increased protection following a standard one-dose challenge, with  $2 \times 10^4$  Py-RAS achieving sterile protection in all animals (Figure 7D). Thus, the Py-RAS trap doses that were fully protective against one-dose ( $2 \times 10^4$ ) and two-dose ( $5 \times 10^2$ ) challenges suggests different thresholds of CD8 $^+$  T cells in each model to completely protect the host.

### CD8 $^+$ T cells and IFN- $\gamma$ are required to protect mice against two-dose challenge

Our data to this point suggests that extra time can help achieve complete protection against LS parasites. Here, we conducted immune cell depletion/blocking studies to determine the relative importance of innate and adaptive immune responses in this protection.

CD8 $^+$  T cells and IFN- $\gamma$  have important roles in combatting *Plasmodium* parasites in the LS<sup>4,5</sup> and leading to sterile protection. To ascertain whether the same mechanism of protection was also acting in a two-dose challenge model, we used monoclonal antibodies (mAbs) to either deplete CD8 $^+$  cells or block action of IFN- $\gamma$  in mice vaccinated once with Py-RAS. Depleting/blocking mAbs were administered intraperitoneally (IP) one day before and one day after challenge dose #1 of the two-dose challenge. Isotype control antibodies were administered to control groups. Blood was collected before and after mAb administration to confirm depletions (Figure S3). Protection was evaluated by blood smears on days 4–10 post-challenge (Figure 8A). Protection was completely abrogated in mice that received anti-CD8 mAbs and was reduced in the anti-IFN- $\gamma$  treated mice (Figure 8B), confirming that CD8 $^+$  T cells and IFN- $\gamma$  are critical for protection in the two-dose challenge model.

CD1d-expressing NKT and  $\gamma\delta$ -T cells comprising the majority of the liver mononuclear cell population could be the initial responders against LS infection.<sup>35,36</sup> They have capacity to produce large quantities of IFN- $\gamma$  upon activation restricting the subsequent LS infection

encountered by host within a short period of time.<sup>32,35,36</sup> There are reports on NKT and  $\gamma\delta$ -T cells playing a role in protecting the host against LS infection by the traditional challenge model.<sup>32,37–39</sup> To evaluate if challenge dose #1 activated these innate immune cells in *Py*-RAS-vaccinated mice, and thereby might also help protect against challenge dose #2, we depleted these cells using anti-CD1d antibodies (Figure 8A). Interestingly, following two-dose challenge of vaccinated mice, CD1d-expressing cells were dispensable for protection (Figure 8B).

As noted above, while the low dose #1 ( $2 \times 10^3$  *Py*-FabB/F) did not induce strong ISG responses in naive mice (Figure 5G), such responses were increased in previously *Py*-RAS immunized mice (Figure 4G). Our experimental setup contrasts with most ISG research in malaria to date, which has been in the setting of naive mice undergoing primary exposure.<sup>31,32,40</sup> In our model, it is likely that antigen-specific CD8<sup>+</sup> T cells in immunized mice are reactivated by dose #1 and serve as the source for accelerated ISG expression compared to naive mice. However, when the interferon- $\alpha/\beta$  receptor (IFNAR) was blocked with mAbs, protection was maintained, indicating that the type I interferon pathway was dispensable for protection (Figure 8B). While we cannot completely rule out a role for type I interferons in the accelerated and more protective immune responses seen in vaccinated mice undergoing two-dose challenge, the dispensable nature of type I interferon signaling in our *Py*-RAS-immunized mice is consistent with another recent study showing that type I interferon signaling impairs spz-induced liver-specific CD8<sup>+</sup> T cell immune memory through a CD8<sup>+</sup> T cell-extrinsic mechanism.<sup>41</sup> The intersection of the innate and adaptive responses is nonetheless complex, and additional future studies will be helpful for unraveling the exact timing and any role (or lack thereof) for ISGs in vaccinated animals at the time of secondary challenge.

## DISCUSSION

A major obstacle in the path of novel antigen discovery for human PE malaria vaccines is that there is no appropriate immunocompetent pre-clinical murine challenge model that mimics the duration of the *Pf*LS in humans. Therefore, our understanding of host-parasite immunological interactions based on murine studies may be temporally misaligned. The short LS duration of *Py* and *Pb* in mice means that the murine immune system is not able to immunologically recapitulate all of the events that occur prior to parasite egress to the erythrocyte stage for *Pf* in humans in the compressed murine parasite timeline. Given this timeline mismatch, careful selection of candidate antigens based on their immunogenicity, protective efficacy and expression timing in *Py/Pb* vs. *Pf* is of utmost importance. Better pre-clinical animal models may help overcome some of these difficulties.

This study reports on a new PE stage murine challenge model that attempts to recapitulate the presumed kinetics of CD8<sup>+</sup> T cells targeting human *Plasmodium* LS infection. CD8<sup>+</sup> T cells play a critical role in conferring sterile protection against malaria during the LS, and the existing pre-clinical mouse model does not make use of the full protective potential of parasite-specific CD8<sup>+</sup> T cells. This new model can help to better understand host-parasite interactions from the CD8<sup>+</sup> T cell immunological perspective and may aid in antigen discovery. In the existing challenge model with short duration LS infection, CD8<sup>+</sup> T cells activate and numerically expand, but the accumulation of these T cells in the liver is too late to participate in killing of infected hepatocytes such that only pre-existing, activated CD8<sup>+</sup> T cells are able to target the parasite. However, in the lengthened LS infection activated and numerically expanding CD8<sup>+</sup> T cells were present and protection was enhanced in mice with these cells present. Under these circumstances, we hypothesize that even memory CD8<sup>+</sup> T cells at sub-optimal levels prior to challenge may be able to contribute to effective parasite killing after expansion.

Few protective antigens such as the circumsporozoite protein (CSP) and the thrombospondin-related adhesive protein (TRAP) have been identified using mouse models.<sup>1,42,43</sup> In humans, these antigens elicit immune responses but their use as sub-unit vaccines in humans have yet to show reliably high protective efficacy.<sup>44,45</sup> Conversely, WPV approaches have been shown to be highly protective in humans,<sup>8,9</sup> but three or more IV doses of spz have always been used in human studies. We previously showed that after the first spz immunization in mice, CD8<sup>+</sup> T cell responses are diminished following subsequent spz immunizations.<sup>46</sup> We have also shown that a single spz immunization dose could be turned protective if preceded by subunit DNA vaccination using appropriate antigens.<sup>10,28</sup> However, human studies rely on preliminary studies in murine models, where antigens selected from the conventional short LS *Plasmodium* challenge models proved to be non-protective in humans. Therefore, the two-dose challenge model was developed to not only provide evidence that single spz vaccinations are protective if increasing numbers of cytotoxic T lymphocyte (CTL) populations can contribute, but also to provide a better model for identification of additional targets for T cells, which may be dismissed using conventional challenge models.

In the two-dose challenge model, subsequent serial doses of late-arresting, genetically attenuated spz (dose #1) followed by WT spz (dose #2) extend the duration of LS antigen exposure in mice to mimic the *Pf* infection observed in humans. Dose #1, intended to elicit recall CD8<sup>+</sup> T cell responses, was designed to resemble spz delivered by one or a few infected mosquitoes as in natural human infection. For example, one study determined that a single mosquito bite delivers 0–1200 spz.<sup>47</sup> The initial dose #1 activates vaccine-induced memory CD8<sup>+</sup> T cells that have time to activate and numerically expand to participate in the killing of the wild-type dose #2 parasites. With this two-dose challenge model, we could not see any influence of dose #2 on the activation and expansion kinetics of CD8<sup>+</sup> T cells in the liver of mice. We could also not see any attenuating effects of dose #1 on the infectivity of the challenge dose #2 in naive mice. One limitation of this study was that the role of antibodies was not assessed, although the IV routing of challenge doses may limit the influence of anti-spz antibodies. In all, this model highlights the impressive efficacy of existing malaria vaccine approaches especially when given two extra days for the cellular immune response to mature. Thus, the two-dose challenge model may be a useful pre-clinical model for studying CD8<sup>+</sup> T cell kinetics and for discovery and evaluation of candidate antigens.

### Limitations of the study

Currently, there is no mouse model and/or murine-infecting *Plasmodium* species that recapitulates the immunological and biological phenomena that occur throughout the duration of normal human liver infection with *Plasmodium* species. This two-dose challenge approach is an approximation of a longer liver stage exposure but may introduce as-yet-unidentified immunological differences compared to a single infection with *P. falciparum* in humans. Also, the study herein focused on total cellular immune responses and not antigen-specific responses, which are more difficult to quantify after a single immunization with whole sporozoites because the resulting T cell frequency remains relatively low for individual antigens. Likewise, the study did not focus on antibodies or comprehensively examine a range of innate immune mediators, though these aspects could also be studied with this model in the future.

### STAR★METHODS

Detailed methods are provided in the online version of this paper and include the following:

- KEY RESOURCES TABLE
- RESOURCE AVAILABILITY
  - Lead contact
  - Materials availability
  - Data and code availability
- EXPERIMENTAL MODEL AND STUDY PARTICIPANT DETAILS
  - Mice
  - *Plasmodium* parasites
- METHOD DETAILS
  - Vaccination and challenge
  - Blood smear endpoints
  - Luciferase-based in-vivo parasite imaging
  - Liver stage *Plasmodium* Type-I ISG RT-PCR and 18S rRNA
  - Flow cytometry
  - Blocking/depletion of immune responses
- QUANTIFICATION AND STATISTICAL ANALYSIS

### SUPPLEMENTAL INFORMATION

Supplemental information can be found online at <https://doi.org/10.1016/j.isci.2023.108489>.

### ACKNOWLEDGMENTS

We thank Will Betz, Eve Chuenchob, Carola Schaefer, Tess Seltzer, Alexis Kaushansky, Ashley Vaughan, Stefan Kappe, and the insectary at the Seattle Children's Research Institute for mosquito and spz production, Deborah Fuller (UW) for gene gun support, Neal Paragas (UW) for IVIS support, BioRender for graphical software, UW vivarium staff, and the NIH Tetramer Core facility.

Funding: This work was partially funded by NIH/NIAID grants (1K08AI097238 and 1R01AI141857 to S.C.M.). The funders had no role in study design, data collection and interpretation, or the decision to submit the work for publication.

### AUTHOR CONTRIBUTIONS

Conceptualization: S.C.M.

Funding acquisition: S.C.M.

Investigation: N.Y., C.P., Z.P.B., B.C.S., F.N.W., K.Z., T.M.O., I.C.T., A.M.S., J.M., M.J.S., R.A.R., and S.C.M.

Methodology: N.Y., C.P., Z.P.B., B.C.S., F.N.W., and S.C.M.

Project administration: S.C.M.

Supervision: S.C.M.

Writing – original draft: N.Y. and S.C.M.

Writing – review and editing: N.Y., C.P., Z.P.B., B.C.S., F.N.W., K.Z., T.M.O., I.C.T., A.M.S., J.M., M.J.S., R.A.R., and S.C.M.

### DECLARATION OF INTERESTS

The authors declare no conflict of interests.

### INCLUSION AND DIVERSITY

We support inclusive, diverse, and equitable conduct of research. One or more of the authors of this paper self-identifies as an underrepresented ethnic minority in their field of research or within their geographical location. One or more of the authors of this paper self-identifies as

a gender minority in their field of research. One or more of the authors of this paper self-identifies as a member of the LGBTQIA+ community. One or more of the authors of this paper received support from a program designed to increase minority representation in their field of research.

Received: March 10, 2023

Revised: October 16, 2023

Accepted: November 14, 2023

Published: November 20, 2023

## REFERENCES

- Keitany, G.J., Sack, B., Smithers, H., Chen, L., Jang, I.K., Sebastian, L., Gupta, M., Sather, D.N., Vignali, M., Vaughan, A.M., et al. (2014). Immunization of mice with live-attenuated late liver stage-arresting *Plasmodium yoelii* parasites generates protective antibody responses to preerythrocytic stages of malaria. *Infect. Immun.* **82**, 5143–5153.
- Doolan, D.L., and Hoffman, S.L. (2000). The complexity of protective immunity against liver-stage malaria. *J. Immunol.* **165**, 1453–1462.
- Lefebvre, M.N., Surette, F.A., Anthony, S.M., Vijay, R., Jensen, I.J., Pewe, L.L., Hancox, L.S., Van Braeckel-Budimir, N., van de Wall, S., Urban, S.L., et al. (2021). Expeditious recruitment of circulating memory CD8 T cells to the liver facilitates control of malaria. *Cell Rep.* **37**, 109956.
- Schofield, L., Villaquiran, J., Ferreira, A., Schellekens, H., Nussenzweig, R., and Nussenzweig, V. (1987). Gamma interferon, CD8+ T cells and antibodies required for immunity to malaria sporozoites. *Nature* **330**, 664–666.
- Weiss, W.R., Sedegah, M., Beaudoin, R.L., Miller, L.H., and Good, M.F. (1988). CD8+ T cells (cytotoxic/suppressors) are required for protection in mice immunized with malaria sporozoites. *Proc. Natl. Acad. Sci. USA* **85**, 573–576.
- Weiss, W.R., and Jiang, C.G. (2012). Protective CD8+ T lymphocytes in primates immunized with malaria sporozoites. *PLoS One* **7**, e31247.
- Fernandez-Ruiz, D., Ng, W., Holz, L.E., Ma, J., Zaid, A., Wong, Y., Lau, L., Mollard, V., Cozijnsen, A., Collins, N., et al. (2016). Liver-resident memory CD8+ T cells form a front-line defense against malaria liver-stage infection. *Immunity* **45**, 889–902.
- Ishizuka, A.S., Lyke, K.E., DeZure, A., Berry, A.A., Richie, T.L., Mendoza, F.H., Enama, M.E., Gordon, I.J., Chang, L.J., Sarwar, U.N., et al. (2016). Protection against malaria at 1 year and immune correlates following PfSPZ vaccination. *Nat. Med.* **22**, 614–623.
- Seder, R.A., Chang, L.J., Enama, M.E., Zephir, K.L., Sarwar, U.N., Gordon, I.J., Holman, L.A., James, E.R., Billingsley, P.F., Gunasekera, A., et al. (2013). Protection against malaria by intravenous immunization with a nonreplicating sporozoite vaccine. *Science* **341**, 1359–1365.
- Watson, F., Shears, M., Matsubara, J., Kalata, A., Seilie, A., Talavera, I.C., Olsen, T., Tsuji, M., Chakravarty, S., Sim, B.K.L., et al. (2022). Cryopreserved sporozoites with and without the glycolipid adjuvant 7DW8-5 protect in prime-and-trap malaria vaccination. *Am. J. Trop. Med. Hyg.* **106**, 1227–1236.
- Carlton, J.M., Angiuoli, S.V., Suh, B.B., Kooij, T.W., Perte, M., Silva, J.C., Ermolaeva, M.D., Allen, J.E., Selengut, J.D., Koo, H.L., et al. (2002). Genome sequence and comparative analysis of the model rodent malaria parasite *Plasmodium yoelii yoelii*. *Nature* **419**, 512–519.
- Gros, P., and Casanova, J.L. (2023). Reconciling mouse and human immunology at the altar of genetics. *Ann. Rev. Immunol.* **41**, 39–71.
- Mestas, J., and Hughes, C.C.W. (2004). Of mice and not men: differences between mouse and human immunology. *J. Immunol.* **172**, 2731–2738.
- Kumar, B.V., Connors, T.J., and Farber, D.L. (2018). Human T cell development, localization, and function throughout life. *Immunity* **48**, 202–213.
- Wherry, E.J., and Ahmed, R. (2004). Memory CD8 T-cell differentiation during viral infection. *J. Virol.* **78**, 5535–5545.
- Gubser, P.M., Bantug, G.R., Razik, L., Fischer, M., Dimeloe, S., Hoenger, G., Durovic, B., Jauch, A., and Hess, C. (2013). Rapid effector function of memory CD8+ T cells requires an immediate-early glycolytic switch. *Nat. Immunol.* **14**, 1064–1072.
- Whitmire, J.K., Eam, B., and Whitton, J.L. (2008). Tentative T cells: memory cells are quick to respond, but slow to divide. *PLoS Pathog.* **4**, e1000041.
- Beura, L.K., Mitchell, J.S., Thompson, E.A., Schenkel, J.M., Mohammed, J., Wijeyesinghe, S., Fonseca, R., Burbach, B.J., Hickman, H.D., Vezys, V., et al. (2018). Intravital mucosal imaging of CD8(+) resident memory T cells shows tissue-autonomous recall responses that amplify secondary memory. *Nat. Immunol.* **19**, 173–182.
- Danahy, D.B., Anthony, S.M., Jensen, I.J., Hartwig, S.M., Shan, Q., Xue, H.H., Harty, J.T., Griffith, T.S., and Badovinac, V.P. (2017). Polymicrobial sepsis impairs bystander recruitment of effector cells to infected skin despite optimal sensing and alarming function of skin resident memory CD8 T cells. *PLoS Pathog.* **13**, e1006569.
- Kohlmeier, J.E., Miller, S.C., Smith, J., Lu, B., Gerard, C., Cookenham, T., Roberts, A.D., and Woodland, D.L. (2008). The chemokine receptor CCR5 plays a key role in the early memory CD8+ T cell response to respiratory virus infections. *Immunity* **29**, 101–113.
- Osborn, J.F., Hobbs, S.J., Mooster, J.L., Khan, T.N., Kilgore, A.M., Harbour, J.C., and Nolz, J.C. (2019). Central memory CD8+ T cells become CD69+ tissue-residents during viral skin infection independent of CD62L-mediated lymph node surveillance. *PLoS Pathog.* **15**, e1007633.
- Müller, K., Gibbins, M.P., Roberts, M., Reyes-Sandoval, A., Hill, A.V.S., Draper, S.J., Matuschewski, K., Silvie, O., and Hafalla, J.C.R. (2021). Low immunogenicity of malaria pre-erythrocytic stages can be overcome by vaccination. *EMBO Mol. Med.* **13**, e13390.
- Patel, H., Yadav, N., Parmar, R., Patel, S., Singh, A.P., Shrivastava, N., and Dalai, S.K. (2017). Frequent inoculations with radiation attenuated sporozoite is essential for inducing sterile protection that correlates with a threshold level of Plasmodia liver-stage specific CD8+ T cells. *Cell. Immunol.* **317**, 48–54.
- Schmidt, N.W., Butler, N.S., Badovinac, V.P., and Harty, J.T. (2010). Extreme CD8 T cell requirements for anti-malarial liver-stage immunity following immunization with radiation attenuated sporozoites. *PLoS Pathog.* **6**, e1000998.
- Yadav, N., Patel, H., Parmar, R., Patidar, M., and Dalai, S.K. (2023). TCR-signals downstream adversely correlate with the survival signals of memory CD8(+) T cells under homeostasis. *Immunobiology* **228**, 152354.
- Moreno-Sabater, A., Pérignon, J.L., Mazier, D., Lavazec, C., and Soulard, V. (2018). Humanized mouse models infected with human *Plasmodium* species for antimalarial drug discovery. *Exp. Opin. Drug Discov.* **13**, 131–140.
- Vaughan, A.M., Sack, B.K., Dankwa, D., Minkah, N., Nguyen, T., Cardamone, H., and Kappe, S.H.I. (2018). A *Plasmodium* parasite with complete late liver stage arrest protects against preerythrocytic and erythrocytic stage infection in mice. *Infect. Immun.* **86**, e00088-18.
- Olsen, T.M., Stone, B.C., Chuenchob, V., and Murphy, S.C. (2018). Prime-and-trap malaria vaccination to generate protective CD8(+) liver-resident memory T cells. *J. Immunol.* **201**, 1984–1993.
- Overstreet, M.G., Cockburn, I.A., Chen, Y.C., and Zavala, F. (2008). Protective CD8 T cells against *Plasmodium* liver stages: immunobiology of an ‘unnatural’ immune response. *Immunol. Rev.* **225**, 272–283.
- Crouse, J., Kalinke, U., and Oxenius, A. (2015). Regulation of antiviral T cell responses by type I interferons. *Nat. Rev. Immunol.* **15**, 231–242.
- Liehl, P., Meireles, P., Albuquerque, I.S., Pinkevych, M., Baptista, F., Mota, M.M., Davenport, M.P., and Prudêncio, M. (2015). Innate immunity induced by *Plasmodium* liver infection inhibits malaria reinfections. *Infect. Immun.* **83**, 1172–1180.
- Miller, J.L., Sack, B.K., Baldwin, M., Vaughan, A.M., and Kappe, S.H.I. (2014). Interferon-mediated innate immune responses against malaria parasite liver stages. *Cell Rep.* **7**, 436–447.
- Nganou-Makamdop, K., and Sauerwein, R.W. (2013). Liver or blood-stage arrest during malaria sporozoite immunization: the later the better? *Trends Parasitol.* **29**, 304–310.
- Gilbert, S.C., Schneider, J., Hannan, C.M., Hu, J.T., Plebanski, M., Sinden, R., and Hill, A.V.

- (2002). Enhanced CD8 T cell immunogenicity and protective efficacy in a mouse malaria model using a recombinant adenoviral vaccine in heterologous prime-boost immunisation regimes. *Vaccine* 20, 1039–1045.
35. Liu, W., and Huber, S.A. (2011). Cross-talk between CD1d-restricted NKT cells and  $\gamma\delta$  cells in T regulatory cell response. *Virology* 43, 8–32.
  36. Hammerich, L., and Tacke, F. (2014). Role of gamma-delta T cells in liver inflammation and fibrosis. *World J. Gastrointest. Pathophys.* 5, 107–113.
  37. Soulard, V., Roland, J., Sellier, C., Gruner, A.C., Leite-de-Moraes, M., Franetich, J.-F., Rénia, L., Cazenave, P.-A., and Pied, S. (2007). Primary infection of C57BL/6 mice with *Plasmodium yoelii* induces a heterogeneous response of NKT cells. *Infect. Immun.* 75, 2511–2522.
  38. Tsuji, M., Mombaerts, P., Lefrançois, L., Nussenzweig, R.S., Zavala, F., and Tonegawa, S. (1994). Gamma delta T cells contribute to immunity against the liver stages of malaria in alpha beta T-cell-deficient mice. *Proc. Natl. Acad. Sci. USA* 91, 345–349.
  39. Zaidi, I., Diallo, H., Conteh, S., Robbins, Y., Kolasny, J., Orr-Gonzalez, S., Carter, D., Butler, B., Lambert, L., Brickley, E., et al. (2017).  $\gamma\delta$  T cells are required for the induction of sterile immunity during irradiated sporozoite vaccinations. *J. Immunol.* 199, 3781–3788.
  40. Liehl, P., Zuzarte-Luis, V., Chan, J., Zillinger, T., Baptista, F., Carapau, D., Konert, M., Hanson, K.K., Carret, C., Lassnig, C., et al. (2014). Host-cell sensors for *Plasmodium* activate innate immunity against liver-stage infection. *Nat. Med.* 20, 47–53.
  41. Minkah, N.K., Wilder, B.K., Sheikh, A.A., Martinson, T., Wegmair, L., Vaughan, A.M., and Kappe, S.H.I. (2019). Innate immunity limits protective adaptive immune responses against pre-erythrocytic malaria parasites. *Nat. Commun.* 10, 3950.
  42. Wang, R., Charoenvit, Y., Corradin, G., Porrozi, R., Hunter, R.L., Glenn, G., Alving, C.R., Church, P., and Hoffman, S.L. (1995). Induction of protective polyclonal antibodies by immunization with a *Plasmodium yoelii* circumsporozoite protein multiple antigen peptide vaccine. *J. Immunol.* 154, 2784–2793.
  43. Lu, C., Song, G., Beale, K., Yan, J., Garst, E., Feng, J., Lund, E., Catteruccia, F., and Springer, T.A. (2020). Design and assessment of TRAP-CSP fusion antigens as effective malaria vaccines. *PLoS One* 15, e0216260.
  44. Kester, K.E., Cummings, J.F., Ofori-Anyinam, O., Ockenhouse, C.F., Krzych, U., Moris, P., Schwenk, R., Nielsen, R.A., Debebe, Z., Pinelis, E., et al. (2009). Randomized, double-blind, phase 2a trial of falciparum malaria vaccines RTS, S/AS01B and RTS, S/AS02A in malaria-naïve adults: safety, efficacy, and immunologic associates of protection. *J. Infect. Dis.* 200, 337–346.
  45. Molano, A., Park, S.-H., Chiu, Y.-H., Nosseir, S., Bendelac, A., and Tsuji, M. (2000). Cutting edge: the IgG response to the circumsporozoite protein is MHC class II-dependent and CD1d-independent: exploring the role of GPIs in NK T cell activation and antimalarial responses. *J. Immunol.* 164, 5005–5009.
  46. Billman, Z.P., Kas, A., Stone, B.C., and Murphy, S.C. (2016). Defining rules of CD8+ T cell expansion against pre-erythrocytic *Plasmodium* antigens in sporozoite-immunized mice. *Malar. J.* 15, 238.
  47. Medica, D.L., and Sinnis, P. (2005). Quantitative dynamics of *Plasmodium yoelii* sporozoite transmission by infected anopheline mosquitoes. *Infect. Immun.* 73, 4363–4369.
  48. Kennedy, M., Fishbaugher, M.E., Vaughan, A.M., Patrapuvich, R., Boonhok, R., Yimamnuaychok, N., Rezakhani, N., Metzger, P., Ponpuak, M., Sattabongkot, J., et al. (2012). A rapid and scalable density gradient purification method for *Plasmodium* sporozoites. *Malar. J.* 11, 421.
  49. Murphy, S.C., Prentice, J.L., Williamson, K., Wallis, C.K., Fang, F.C., Fried, M., Pinzon, C., Wang, R., Talley, A.K., Kappe, S.H.I., et al. (2012). Real-time quantitative reverse transcription PCR for monitoring of blood-stage *Plasmodium falciparum* infections in malaria human challenge trials. *Am. J. Trop. Med. Hyg.* 86, 383–394.
  50. Yadav, N., Parmar, R., Patel, H., Patidar, M., and Dalai, S.K. (2022). Infectious sporozoite challenge modulates radiation attenuated sporozoite vaccine-induced memory CD8+ T cells for better survival characteristics. *Microbiol. Immunol.* 66, 41–51.
  51. Patel, H., Althubaiti, N., Parmar, R., Yadav, N., Joshi, U., Tyagi, R.K., Krzych, U., and Dalai, S.K. (2019). Parasite load stemming from immunization route determines the duration of liver-stage immunity. *Parasite Immunol.* 41, e12622.

STAR★METHODS

KEY RESOURCES TABLE

REAGENT or RESOURCE	SOURCE	IDENTIFIER
<b>Antibodies</b>		
Anti-mouse CD3e	BD Biosciences	Cat# 565992, RRID: AB_2739443
Anti-mouse CD4	BioLegend	Cat# 100430 (also 100429), RRID: AB_493699
Anti-mouse CD8 $\alpha$	BD Biosciences	Cat# 563898, RRID: AB_2738474
Anti-mouse CD44	BioLegend	Cat# 103016 (also 103015), RRID: AB_493679
Anti-mouse CD62L	BD Biosciences	Cat# 560516, RRID: AB_1645257
Anti-mouse CD69	BD Biosciences	Cat# 563030, RRID: AB_2737963
Anti-mouse KLRG1	BioLegend	Cat# 138418 (also 138417), RRID: AB_2563015
Mouse CD1d	NIH-Tetramer core	<a href="https://tetramer.yerkes.emory.edu/">https://tetramer.yerkes.emory.edu/</a>
Anti-mouse CD16/32	BD Biosciences	Cat# 553140, RRID:AB_394655
Anti-mouse CD8 $\alpha$	Bio X Cell	Cat# BE0061 (also BE0061-100MG, BE0061-1MG, BE0061-25MG, BE0061-50MG, BE0061-5MG, BP0061-100MG, BP0061-25MG, BP0061-50MG, BP0061-5MG), RRID: AB_1125541
IgG2b isotype control, anti-keyhole limpet hemocyanin	Bio X Cell	Cat# BE0090 (also BE0090-100MG, BE0090-1MG, BE0090-25MG, BE0090-50MG, BE0090-5MG, BP0090-100MG, BP0090-25MG, BP0090-50MG, BP0090-5MG), RRID: AB_1107780
Anti-mouse IFN $\gamma$	Bio X Cell	Cat# BE0055 (also BE0055-100MG, BE0055-1MG, BE0055-25MG, BE0055-50MG, BE0055-5MG, BP0055-100MG, BP0055-25MG, BP0055-50MG, BP0055-5MG), RRID: AB_1107694
Anti-mouse IFNAR-1	Leinco Technologies	Cat# I-401, RRID:AB_2491621
IgG1 Isotype Control	Leinco Technologies	Cat# I-536, RRID: AB_2737545
Anti-mouse CD1d	Bio X Cell	Cat# BE0000 (also BE0000-100MG, BE0000-1MG, BE0000-25MG, BE0000-50MG, BE0000-5MG), RRID: AB_1107568
<b>Chemicals, peptides, and recombinant proteins</b>		
Percoll® PLUS	Millipore Sigma	Cat # GE17-5445-01
D-Luciferin	Goldbio	Cat # LUCK-1G
Nuclisens Lysis Buffer	bioMérieux	Cat # 280134
Accudenz	Accurate	Cat # AN7050
<b>Critical commercial assays</b>		
One Step AgPath RT-PCR kit	Fisher Scientific	Cat # Agpath AM1005
Zombie NIR™ Fixable Viability Kit	BioLegend	Cat # 423105

(Continued on next page)



**Continued**

REAGENT or RESOURCE	SOURCE	IDENTIFIER
<i>Experimental models: Organisms/strains</i>		
Mouse: BALB/cJ	The Jackson Laboratory	Strain #:000651 RRID: IMSR_JAX:000651
Mouse: C57BL/6J	The Jackson Laboratory	Strain #:000664 RRID: IMSR_JAX:000664
Mosquito: <i>Anopheles stephensi</i>	Seattle Children's Research Institute, Seattle	N/A
Parasite: <i>Plasmodium yoelii</i> 17XNL (wild type)	Seattle Children's Research Institute, Seattle	N/A
Parasite: <i>Plasmodium yoelii</i> 17XNL (Luc)	Seattle Children's Research Institute, Seattle	N/A
Parasite: <i>Plasmodium yoelii</i> 17XNL ( <i>fabB/F</i> -/- knockout)	Seattle Children's Research Institute, Seattle	N/A
<i>Oligonucleotides</i>		
<i>Ifit1</i> (forward: CCTTTACA- GCAACCATGGGAGA)	Integrated DNA Technologies, Inc.	N/A
<i>Ifit1</i> (reverse: GCAGCTTCCATGTGAAGTGAC)	Integrated DNA Technologies, Inc.	N/A
<i>Ifit44</i> (forward: TC-GATTCCATGAAACCAATCAC)	Integrated DNA Technologies, Inc.	N/A
<i>Ifit44</i> (reverse: CAAATGCAGAATGCCATGTTTT)	Integrated DNA Technologies, Inc.	N/A
<i>Recombinant DNA</i>		
pUb.3-CSP plasmid ( <i>Py</i> -CSP plasmid)	Ref. <sup>28</sup>	N/A
pUb.3 plasmid (Vector plasmid)	Ref. <sup>28</sup>	N/A
<i>Software and algorithms</i>		
FlowJo software	BD Biosciences	<a href="https://www.flowjo.com/">https://www.flowjo.com/</a>
GraphPad prism	GraphPad	<a href="https://www.graphpad.com/">https://www.graphpad.com/</a>
Living Image 3.0®	Perkin-Elmer	<a href="https://www.perkinelmer.com/category/in-vivo-imaging-software">https://www.perkinelmer.com/category/in-vivo-imaging-software</a>
<i>Other</i>		
<i>In-vivo</i> bioluminescent imager	Xenogen IVIS Spectrum, Caliper Life Sciences/ Perkin Elmer	<a href="https://www.perkinelmer.com/Product/ivis-instrument-spectrum-120v-andor-c-124262">https://www.perkinelmer.com/Product/ivis-instrument-spectrum-120v-andor-c-124262</a>
EasyMag system	BioMérieux	<a href="https://www.biomerieux-usa.com/clinical/nuclisens-easymag">https://www.biomerieux-usa.com/clinical/nuclisens-easymag</a>

**RESOURCE AVAILABILITY**

**Lead contact**

Further information and requests should be directed to the lead contact, Sean Murphy ([murphysc@uw.edu](mailto:murphysc@uw.edu)).

**Materials availability**

All unique/stable reagents generated in this study are available from the [lead contact](#) with a completed Materials Transfer Agreement.

**Data and code availability**

- Data: Flow cytometry, RT-PCR, and protection data reported in this paper will be shared by the [lead contact](#) upon request.
- Code: This paper does not report original code.
- Any additional information required to reanalyze the data reported in this paper is available from the [lead contact](#) upon request.

**EXPERIMENTAL MODEL AND STUDY PARTICIPANT DETAILS**

**Mice**

Female BALB/cJ and C57BL/6 mice (4-6 weeks old) were obtained from Jackson Laboratories (Barr Harbor, ME), housed in an IACUC-approved animal facility at the University of Washington and used under an approved IACUC protocol 4317-01 (SCM).

### Plasmodium parasites

Wild-type *P. yoelii* (Py-WT), unattenuated GFP/luciferase-expressing *P. yoelii* 17XNL (Py-Luc), and genetically attenuated, late-arresting, *fabB/F*-/- knockout *P. yoelii* (Py-FabB/F) spz were harvested 14–16 days after an infectious blood meal by salivary gland dissection from infected *A. stephensi* mosquitoes reared at the Center for Mosquito Production and Malaria Infection Research (CeMPMIR) at the Center for Global Infectious Disease Research (CGIDR), Seattle Children's Research Institute. Following dissection, spz purification was conducted prior to irradiation using the Accudenz gradient method.<sup>48</sup> Briefly, after layering one-part salivary gland spz suspended in Schneider's media over three parts 17% (w/v) Accudenz and centrifugation as reported, the top one-third of the gradient was transferred into 1.6 mL tubes and centrifuged at 13,300 x g for 4 minutes.<sup>48</sup> Pellets from these tubes were combined, diluted with at least four parts of Schneider's medium and the spz were counted using a hemocytometer.

## METHOD DETAILS

### Vaccination and challenge

For spz immunizations, radiation-attenuation of Py spz (Py-RAS) was done by exposing wild-type parasite (Py-WT) to 10,000 rads of X-rays (Rad Source, Suwanee, GA). For two-dose spz challenge, Py-FabB/F and Py-WT were sequentially used; in some cases, Py-Luc was substituted for Py-WT in order to image the liver burden of the unattenuated challenge dose. Immunization and challenge spz were administered intravenously (retro-orbital) in a volume of 100  $\mu$ L per mouse. Dosages are indicated in separate experiments. For DNA vaccinations, DNA encoding the antigen of interest, was delivered by gene gun as described.<sup>28</sup>

### Blood smear endpoints

From day 3 post-challenge, blood collected from mice by tail prick was smeared on glass slides, fixed with methanol and stained with Giemsa stain for detection of blood-stage *Plasmodium* parasites. Blood smears were monitored for the presence of parasites under an oil-immersion lens (1000X total magnification) and blood collection was stopped either at day 10 post-challenge or when parasitemia reached 1%. Animals were humanely euthanized upon reaching 1% parasitemia or at the end of the study.

### Luciferase-based in-vivo parasite imaging

Parasite burden in the liver was measured prior to sacrifice using an *in-vivo* bioluminescent imager (Xenogen IVIS Spectrum, Caliper Life Sciences, USA) as described.<sup>28</sup> Briefly, mice previously infected with Py-Luc spz were injected IP with firefly D-Luciferin prior to undergoing isoflurane anesthesia. Bioluminescence was acquired and measured as previously reported using a 1-minute acquisition time. IVIS images were quantitatively evaluated using Living Image 3.0 software (Perkin-Elmer) with ROIs placed around the abdominal area overlying the liver. ROI measurements were recorded in total flux (p/sec/cm<sup>2</sup>/sr).

### Liver stage Plasmodium Type-I ISG RT-PCR and 18S rRNA

Forty-two to forty-four hours post-challenge, mice were sacrificed, and half of the total liver was excised and pulverized by bead beating in 5 mL Nuclisens Lysis Buffer (bioMérieux). Total RNA was extracted by processing 100  $\mu$ L of the NucliSens buffer-treated sample diluted 1:10 in Nuclisens Lysis Buffer on the EasyMag system (bioMérieux) as described for whole blood.<sup>49</sup> RNA was subjected to RT-PCR using the One Step AgPath RT-PCR kit (Fisher Scientific). *Plasmodium* 18S rRNA detection was done using a predesigned HEX-labeled mouse GAPDH RT-PCR assay (IDT Inc., Coralville, IA) multiplexed with a Pan-*Plasmodium* assay as described.<sup>10</sup> Type-I interferon stimulated genes (ISGs) were evaluated using *Ifit1* (forward: CCTTTACA- GCAACCATGGGAGA; reverse: GCAGCTCCATGTGAAGTGAC) and *Ifit44* (forward: TC-GATTCCATGAAACCAATCAC; reverse: CAAATGCAGAATGCCATGTTTT) primers. Data were normalized to mouse GAPDH and transformed to relative log<sub>10</sub> values to compare log<sub>10</sub> copy number reduction versus the control group.

### Flow cytometry

Liver lymphocytes were isolated as previously described.<sup>50,51</sup> Briefly, livers perfused with PBS containing 2 mM EDTA were dissociated by passing through 200  $\mu$ m cell strainers and rinsed with RPMI supplemented with glutamine and 5% fetal bovine serum (FBS) on ice. After separating gross hepatocytes by centrifugation, monocytes from the resulting cell suspension were isolated using Percoll (Millipore Sigma) density gradient method. Red blood cells were lysed using RBC lysis buffer and the final cell pellets were resuspended in 100  $\mu$ L staining buffer (PBS with 2mM EDTA + 0.5% FBS). Cells were blocked with Fc CD16/32 (clone 2.4G2, BD) containing 1:1000 Zombie viability dye (cat # 423105, BioLegend) for 30 minutes. Surface staining was done by incubating cells for 20 minutes on ice with an antibody cocktail specific to cell surface markers (Table S1). Antibodies were diluted in staining buffer containing 50% Brilliant buffer by volume. Cells were then washed with staining buffer, fixed with 1% formaldehyde reagent prepared in stain buffer. Stained cells were acquired in LSRII machine (BD Biosciences) and analyzed using FlowJo software (v10.8.1).

### Blocking/depletion of immune responses

Immune cell depletion or blocking studies were conducted using the antibodies as depicted in Table S2. Antibodies were diluted in PBS were administered intraperitoneally on days -1 and +1 relative to dose #1 (Py-FabB/F) of the two-dose challenge.

### QUANTIFICATION AND STATISTICAL ANALYSIS

Data are presented as the mean  $\pm$  SEM. All comparisons of liver burden (IVIS), ISG expression levels and cell frequency were by the non-parametric Mann-Whitney *U* test (Student's *t*-test). Protection data were analyzed using Fisher's exact test. Flowcytometry data were analyzed using FlowJo version 10.8.1. Statistical significance was defined as  $P < 0.05$ . Prism GraphPad Prism 9.1.2 Software (San Diego, CA) was used for all calculations.